Properties of spontaneous Ca^{2+} transients recorded from interstitial cells of Cajal-like cells of the rabbit urethra *in situ*

Hikaru Hashitani and Hikaru Suzuki

Department of Regulatory Cell Physiology, Nagoya City University Graduate School of Medical Sciences, Nagoya 467-8601, Japan

Interstitial cells of Cajal-like cells (ICC-LCs) in the urethra may act as electrical pacemakers of spontaneous contractions. However, their properties *in situ* and their interaction with neighbouring urethral smooth muscle cells (USMCs) remain to be elucidated. To further explore the physiological role of ICC-LCs, spontaneous changes in $[Ca^{2+}]_i$ (Ca^{2+} transients) were visualized in fluo-4 loaded preparations of rabbit urethral smooth muscle. ICC-LCs were sparsely distributed, rather than forming an extensive network. Ca^{2+} transients in ICC-LCs had a lower frequency and a longer half-width than those of USMCs. ICC-LCs often exhibited Ca^{2+} transients synchronously with each other, but did not often show a close temporal relationship with Ca^{2+} transients in USMCs. Nicardipine (1 μM) suppressed Ca^{2+} transients in USMCs but not in ICC-LCs. Ca^{2+} transients in ICC-LCs were abolished by cyclopiazonic acid (10 μM), ryanodine (50 μM) and caffeine (10 mM) or by removing extracellular Ca^{2+}, and inhibited by 2-aminoethoxydiphenyl borate (50 μM) and 3-morpholino-sydnonimine (SIN-1; 10 μM), but facilitated by increasing extracellular Ca^{2+} or phenylephrine (1–10 μM). These results indicated that Ca^{2+} transients in urethral ICC-LCs *in situ* rely on both Ca^{2+} release from intracellular Ca^{2+} stores and Ca^{2+} influx through non-L-type Ca^{2+} channel pathways. ICC-LCs may not act as a coordinated pacemaker electrical network as do ICC in the gastrointestinal (GI) tract. Rather they may randomly increase excitability of USMCs to maintain the tone of urethral smooth muscles.

(Resubmitted 17 May 2007; accepted after revision 29 June 2007; first published online 5 July 2007)

Corresponding author H. Hashitani: Department of Regulatory Cell Physiology, Nagoya City University, Graduate School of Medical Sciences, Nagoya 467-8601, Japan. Email: hasitani@med.nagoya-cu.ac.jp

Smooth muscles in the urethra generate spontaneous contractions, which are tonically augmented by neurally released noradrenaline (NAd) through the activation of α_1-adrenoceptors, to maintain a sustained tone (Andersson & Wein, 2004). Underlying these contractions is spontaneous electrical activity, termed spontaneous transient depolarizations (STDs) and slow waves (Hashitani *et al.* 1996; Hashitani & Edwards, 1999). STDs are initiated by mean of the spontaneous release of Ca^{2+} from intracellular stores, which activates Ca^{2+}-activated chloride channels. Summed STDs result in larger depolarizations which activate L-type Ca^{2+} channels to compose the plateau phase of slow waves and contract smooth muscles (Hashitani *et al.* 1996; Hashitani & Edwards, 1999).

Although this spontaneous activity was originally assumed to be generated within USMCs themselves, extensive research using isolated cells taken from the urethra has now revealed that this 'myogenic' activity may originate from ICC-LCs. Isolated ICC-LCs but not USMCs

exhibit spontaneous Ca^{2+} oscillations and spontaneous transient inward currents (STICs), which depend on Ca^{2+} release from intracellular Ca^{2+} stores and the subsequent activation of Ca^{2+}-activated chloride channels, respectively (Sergeant *et al.* 2000, 2001; Johnston *et al.* 2005). Therefore, ICC-LCs may be responsible for the initiation and propagation of electrical activity recorded from intact tissue preparations of the urethra, and act as electrical pacemaker cells as do ICC located in the myenteric region (ICC-MY) of the GI tract (Dickens *et al.* 1999; Sanders *et al.* 2006).

The frequencies of STDs and of STICs recorded in isolated urethral ICC-LCs are increased by bath-applied NAd (Sergeant *et al.* 2000, 2002). Moreover, spontaneous Ca^{2+} transients recorded from isolated ICC-LCs are diminished by either nitric oxide (NO) or cyclic GMP (Sergeant *et al.* 2006b). This is consistent with the effects of NAd and sodium nitroprusside, an NO donor, on the frequency of slow waves recorded in the intact circular smooth muscles of the rabbit urethra (Hashitani *et al.*

1996), suggesting that ICC-LCs may also play an important role in the neurally mediated regulation of spontaneous excitation as do intramuscular ICC (ICC-IM) in the GI tract (Ward *et al.* 2000; Suzuki *et al.* 2003). This hypothesis was further supported by a recent report showing frequent points of contact between Kit-positive ICC-LCs and nerves, particularly nitrergic nerves (Lyons *et al.* 2007).

Since the primary step of spontaneous activity in the urethra is Ca^{2+} release from intracellular stores in ICC-LCs, blockade of sarco/endoplasmic reticulum Ca^{2+}-ATPase (SERCA) with cyclopiazonic acid (CPA) would be expected to suppress urethral smooth muscle contractions. However, CPA, which has been shown to abolish STICs in isolated ICC-LCs (Sergeant *et al.* 2001), increased the amplitude and duration of spontaneous contractions in a majority of preparations of rabbit urethra (Hashitani *et al.* 2006). Similar heterogeneity was observed for the effects of CPA on slow waves or spontaneous Ca^{2+} transients in the rabbit urethra. Thus, it is important to know if CPA effectively prevents spontaneous activity in urethral ICC-LCs *in situ*, and thus if ICC-LCs may be able to generate pacemaking activity via Ca^{2+} store-independent mechanisms.

The mechanical characteristics of the urethral smooth muscles, which display sustained tone (Bridgewater *et al.* 1993), are clearly different from those of GI smooth muscles, which generate phasic contractions for peristalsis. Therefore, even though ICC-LCs in the urethra may act as primary pacemaker cells, as do ICC in the GI tract, either the initiation or propagation of spontaneous activity in the urethra may not be similar to that in the GI tract where highly coordinated oscillators, i.e. ICC-MY and ICC-IM, drive the bulk of the smooth muscles within the wall.

The aim of the present study was to visualize spontaneous Ca^{2+} transients in ICC-LCs of the rabbit urethra *in situ* to compare their properties with those of USMCs *in situ* and also with previously reported characteristics of isolated ICC-LCs. We also investigated the mechanisms underlying the initiation and propagation of the spontaneous Ca^{2+} transients in the urethra, focusing particularly on the interactions between ICC-LCs and USMCs.

Methods

Tissue preparation

Male rabbits, weighing 2–3 kg, were killed by exsanguinations under pentobarbitone anaesthesia. This procedure has been approved by the animal experimentation ethics committee of the Physiological Society of Japan. The urethra and bladder were removed, and the urethra was dissected free of the bladder approximately 3 cm distal of the bilateral ureter entry. The dorsal wall of the urethra was then opened longitudinally and the mucosa and periurethral connective tissues were dissected away. The outer striated muscle and longitudinal smooth muscle were then carefully removed leaving the circular muscle layers intact. Since the division into circular and longitudinal smooth muscle layers is not as clear as in the GI tract wall, circular muscle sections lying close to the submucosal border were used for experiments.

Immunohistochemistry

To identify cells expressing Kit immunoreactivity, preparations which contained several muscle bundles were incubated for 1 h in nominally Ca^{2+} free physiological salt solution (PSS) containing rat monoclonal antibodies raised against the Kit protein (ACK-2, diluted 1 : 100, Cymbus Biotechnology Ltd, Hampshire, UK). The tissue was washed and then incubated for another 1 h in anti-rat IgG antibody labelled with a fluorescent marker (IgG-Alexa Fluor 488, diluted 1 : 250, Molecular Probes, OR, USA). After washing with PSS, preparations were observed using an inverted fluorescence microscope (IX70, Olympus) equipped with an electron multiplier CCD camera (C9100, Hamamatsu Photonics). Kit-positive ICC-LCs were also viewed under Nomarski optics. On some occasions, preparations which had been incubated for ACK-2 with IgG-Alexa Fluor 488, were subsequently loaded with fura-2 AM (10 μM; Molecular Probes) as previously described (Hashitani *et al.* 2006). Preparations, loaded with fura-2, were illuminated with ultraviolet light (wavelengths 340 and 380 nm) and the emission fluorescence was measured through a barrier filter (peak transmission 510 nm), using a micro photoluminescence measurement system (Aquacosmos, Hamamatsu Photonics).

Intracellular calcium measurements

To visualize changes in the concentration of intracellular calcium ($[Ca^{2+}]_i$; Ca^{2+} transients) recorded from USMCs and ICC-LCs, different loading conditions, i.e. 'normal' and 'light' loadings, respectively, were applied. For visualizing Ca^{2+} transients in circular USMCs, preparations were pinned out on a Sylgard plate (silicone elastomer, Dow Corning Corp., Midland, MI, USA) which had a window of some 1.5 mm × 3 mm in the centre. To minimize tissue distortion due to smooth muscle contractions, preparations were stretched radially using 15–20 L-shaped tungsten wires (20 μm in diameter). After 30 min incubation with warmed (36°C) PSS, spontaneous muscle contractions were visually detected, and preparations were then incubated in low-Ca^{2+} PSS ($[Ca^{2+}]_o = 0.1$ mM) containing 3–5 μM fluo-4 AM (FluoroPure™ grade special packaging, Molecular Probes) and cremophor EL (0.01%, Sigma) for 45–60 min at room temperature ('normal' loading). Following

incubation, the preparations were superfused with dye-free, warmed (36°C) PSS at a constant flow rate (about 2 ml min^{-1}) for 30 min

To visualize Ca^{2+} signals in ICC-LCs of the rabbit urethra *in situ*, preparations were incubated in low Ca^{2+} physiological salt solution (PSS) ([Ca^{2+}]$_o$ = 0.1 mM) containing fluo-4 AM (0.1–1 μM) and cremophor EL (0.01%) for 15–30 min at 36°C ('light' loading). Although USMCs' Ca^{2+} signals were hardly detected in this loading condition, increasing [Ca^{2+}]$_o$ from 0.1 mM to 0.5 mM enhanced USMCs' Ca^{2+} signals to a measurable level, and thus allowed the investigation of temporal relationships of Ca^{2+} signals between ICC-LCs and USMCs. Following incubation, the preparations were superfused with dye-free, warmed (36°C) PSS at a constant flow (about 2 ml min^{-1}) for 30 min.

The recording chamber was mounted on the stage of an inverted fluorescence microscope (IX70, Olympus) equipped with an electron multiplier CCD camera (C9100, Hamamatsu Photonics) and a high speed scanning poly-chromatic light source (C7773, Hamamatsu Photonics). Preparations were viewed under either a water-immersion objective (UPlanApo 60, Olympus) or an air objective (UPlanApo 20, Olympus) and illuminated at 495 nm. For the ×60 objective, the Sylgard plate was turned over and then placed at the bottom of the recording chamber so that the preparation now faced the glass bottom of the chamber. The fluorescence emission in a variable sized rectangular window was measured through a barrier filter above 515 nm, and images were obtained every 35–200 ms (frame interval) with an exposure time of 17.4–58.7 ms using a micro-photoluminescence measurement system (Aquacosmos, Hamamatsu Photonics). Relative changes in [Ca^{2+}]$_i$ were expressed as the ratio (F/F_0) of the fluorescence generated by an event (F) against baseline (F_0).

Isometric tension recordings

To detect changes in muscle tension and [Ca^{2+}]$_i$ in USMCs simultaneously, one end of the preparations was pinned out on a Sylgard plate, and the other end was tied by a nylon thread which connected to a force transducer. Isometric tension changes were digitized using a Digidata 1200 interface and stored on a personal computer for later analysis.

Solutions and drugs

The ionic composition of PSS was as follows (mM): NaCl, 119; KCl, 5.0; CaCl$_2$, 2.5; MgCl$_2$, 2.0; NaHCO$_3$, 25.0; NaH$_2$PO$_4$, 1.0; and glucose, 11.0. The solution was bubbled with 95% O$_2$ and 5% CO$_2$ to maintain pH in the recording bath at approximately 7.4. High Ca^{2+} solution or nominally Ca^{2+} free solution was prepared by either increasing or omitting CaCl$_2$ from the composition of PSS, respectively.

Drugs used were 3-morpholino-sydnonimine (SIN-1) hydrochloride, 2-aminoethoxydiphenyl borate (2-APB), caffeine, cyclopiazonic acid (CPA), nicardipine, phenylephrine hydrochloride and ryanodine (all from Sigma, St Louis, MO, USA). These drugs were dissolved in distilled water except CPA, nicardipine, 2-APB and ryanodine, which were dissolved in dimethyl sulphoxide (DMSO). Caffeine was directly dissolved in PSS to obtain its final concentration. The final concentration of these solvents in physiological saline did not exceed 1 : 1000.

Calculations and statistics

Measured values are expressed as means ± standard deviation. Statistical significance was tested using Student's *t* test, and probabilities of less than 5% were considered significant. The synchronicity of Ca^{2+} signals between ICC-LC and either ICC-LC or USMC were analysed using the cross-correlation function of Clampfit 10 software (Axon Instruments–Molecular Devices, Union City, CA, USA).

Results

Identification of ICC-LCs *in situ* in the rabbit urethra

Consistent with recent reports (McHale *et al.* 2006; Lyons *et al.* 2007), Kit-positive cells which we have designated as ICC-LCs, were sparsely distributed in the rabbit urethral preparations, being situated predominately within the connective tissue between the smooth muscle bundles. ICC-LCs were also scattered amongst the smooth muscle cells within muscle bundles. ICC-LCs had either spindle-shaped cell bodies, some 60–100 μm in length and less than 10 μm in width (Fig. 1*Aa*), or stellate-shaped cell bodies with a few processes (Fig. 1*Ba*). The general morphology of ICC-LCs which had been identified by their Kit immunoreactivity was also visualized using Nomarski optics (Fig. 1*Ab* and *Bb*).

In preparations which had been loaded with Kit antibody and fura-2, ICC-LCs identified by their immunoreactivity for Kit (Fig. 1*Ca*) generally had a higher F_{340} fluorescence than that of USMCs (Fig. 1*Cb*), whilst having similar F_{380} fluorescence to that of USMCs (Fig. 1*Cc*). ICC-LCs had higher basal fluorescence in either fura-2 or fluo-4 loaded preparations, which were not stained with Kit antibody suggesting that the Kit antibody little affected ICC-LCs viability.

For the following functional studies, ICC-LCs were identified by their high basal fluorescence, general morphology, location and slower Ca^{2+} signals (see details below). Therefore, we were not able to tell whether or not all ICC-LCs were Kit-positive, and thus could not exclude

the possibility that we have investigated heterogeneous populations of cells.

Spontaneous Ca²⁺ transients recorded from USMCs of the rabbit urethra

Under 'normal' fluo-4 loading conditions, USMCs generated spontaneous Ca^{2+} transients at a frequency of $10.8 \pm 4.3 \, min^{-1}$ ($n = 24$). USMC Ca^{2+} transients had an amplitude of $0.36 \pm 0.12 \, F/F_0$ and a half-amplitude duration (half-width) of $0.69 \pm 0.23 \, s$ ($n = 24$). These values of the frequency and half-width were similar to those of fura-2 loaded urethra preparations (Hashitani *et al.* 2006). USMC Ca^{2+} transients occurred either as non-propagated Ca^{2+} transients (Fig. 2*Aa*) or intercellular Ca^{2+} waves within a muscle bundle (Fig. 2*Ab*). Unlike intercellular Ca^{2+} waves in detrusor smooth muscle

Figure 1. Identification of ICC-LCs in the rabbit urethra
Panels *a* show fluorescent images of ICC-LCs in the rabbit urethra stained using ACK2 antibody against Kit labelled with Alexa 488. Panels *b* show micrographs of preparations viewed with Nomarski optics. *A*, ICC-LC (arrow head) which had a spindle-shaped cell body is shown lying in parallel with a muscle bundle (SMC). *B*, another ICC-LC having a stellate-shaped cell body is shown located in the connective tissue between the muscle bundles. *C*, in a different preparation, which had been loaded with fura-2, ICC-LCs identified by immunoreactivity against Kit (*a*) had higher F_{340} fluorescence than neighbouring smooth muscle cells (SMC, *b*), whilst having similar F_{380} fluorescence (*c*).

bundles of the guinea-pig bladder (Hashitani *et al.* 2001), the Ca^{2+} waves originated from a single site often failed to spread across muscle bundles (Fig. 2*B*).
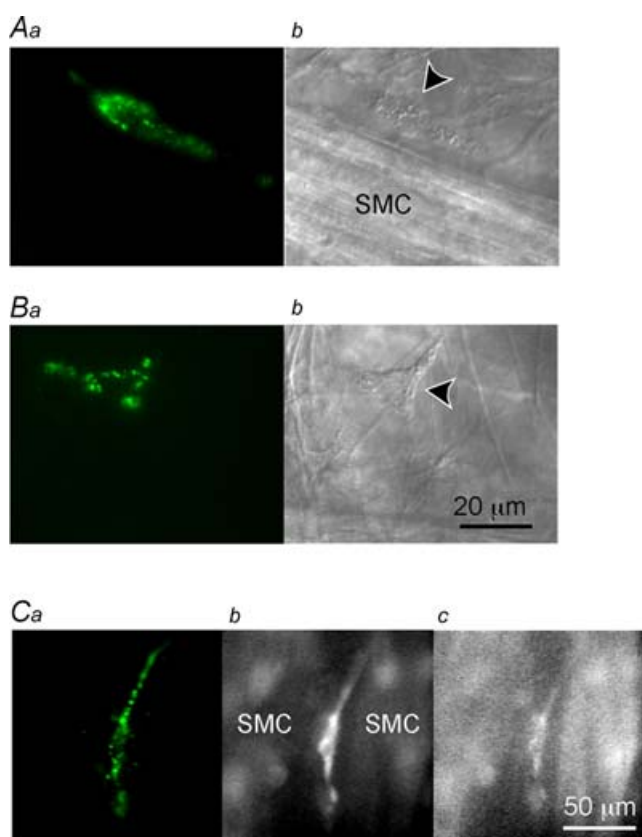
To investigate the correlation between spontaneous USMC Ca^{2+} transients and muscle contractions, changes in muscle tension were simultaneously recorded with $[Ca^{2+}]_i$. Unloaded urethral preparations generated spontaneous contractions $14.3 \pm 3.2 \, min^{-1}$ ($n = 6$). After 'normal' fluo-4 loading, the preparations exhibited spontaneous contractions $13.7 \pm 2.8 \, min^{-1}$, and these values were not significantly different from control values ($P > 0.4$, $n = 6$), indicating that 'normal' fluo-4 loading did not disrupt USMC activity. Although the frequency of spontaneous contractions were similar to those of USMC Ca^{2+} transients, there was no correlation between muscle contractions and Ca^{2+} transients in any particular muscle bundle within the preparations, presumably arising from a low synchronicity between bundles.

After 'normal' loading conditions ICC-LCs were readily identified by their high basal fluorescence intensity (see Fig. 1*C*) and seen either to be separately distributed or to form linear connections with a few neighbouring ICC-LCs. Under these conditions ICC-LCs seldom displayed spontaneous Ca^{2+} transients.

Spontaneous Ca²⁺ transients recorded from ICC-LCs of the rabbit urethra

To visualize Ca^{2+} transients in ICC-LCs more consistently, the 'light' loading of the fluo-4 protocol was used. Both spindle- (Fig. 3*Aa*) and stellate-shaped (Fig. 3*Ba*) ICC-LCs generated spontaneous Ca^{2+} transients. Spontaneous Ca^{2+} transients recorded from spindle-shaped ICC-LCs occurred at a rate of $0.7–9 \, min^{-1}$ ($3.1 \pm 1.6 \, min^{-1}$, $n = 39$) and an amplitude of $0.75 \pm 0.31 \, F/F_0$ ($n = 39$, Fig. 3 Ab). Their half-width ranged between 1.9 and 12.6 s (mean $3.9 \pm 1.8 \, s$, $n = 39$, Fig. 3*Ca*), significantly longer than the half-widths of Ca^{2+} transients in USMCs ($0.69 \pm 0.23 \, s$, $n = 24$, $P < 0.05$, Fig. 3*Cb*), which were measured under 'normal' loading condition. Stellate-shaped ICC-LCs generated spontaneous Ca^{2+} transients at a rate of $0.96–7.5 \, min^{-1}$ ($3.2 \pm 1.8 \, min^{-1}$, $n = 24$), which had an amplitude of $0.79 \pm 0.35 \, F/F_0$ ($n = 24$, Fig. 3*Bb*) and half-width ranging between 1.9 and 6.1 s (mean $3.7 \pm 1.3 \, s$, $n = 24$). These values were not significantly different from those of Ca^{2+} transients in spindle-shaped ICC-LCs ($P > 0.2$).

In 22 preparations where more than two ICC-LCs generated Ca^{2+} transients within a field of view ($135 \, \mu m \times 135 \, \mu m$, $\times 60$ objective), the temporal relationship between ICC-LCs was examined. In 17 out of 22 preparations, pairs of ICC-LCs exhibited synchronous Ca^{2+} transients (Fig. 4*A*, *B* and *D*). Figure 4*C* illustrates the cross-correlogram for one of these pairs of ICC-LCs generating synchronous Ca^{2+} transients, clearly

demonstrating a peak near lag period zero and therefore a close temporal correlation (Fig. 4C). In the remaining five preparations, no temporal relationship was observed between pairs of ICC-LCs (Fig. 4D).

Interaction between ICC-LCs and USMCs in the rabbit urethra

In 21 preparations, spontaneous Ca^{2+} transients in ICC-LCs were observed simultaneously with those of USMCs within a field of view ($\times 60$ objective). Under 'light' loading conditions, USMCs generated spontaneous Ca^{2+} transients at a frequency of 8.7 ± 3.5 min^{-1}, and had an amplitude of 0.28 ± 0.15 F/F_0 and a half-width of 0.62 ± 0.12 s ($n = 28$). In five preparations, ICC-LCs and USMCs generated synchronous Ca^{2+} transients (Fig. 5A and B). A cross-correlogram for ICC-LCs and USMCs showed a peak near lag period zero, suggesting a close temporal correlation between the two cell types (Fig. 5C). The peak correlation values were consistently smaller than those of the correlograms for pairs of ICC-LCs as the configuration of USMC Ca^{2+} transients was fairly different from those of ICC-LCs. In the remaining 16 preparations, USMCs generated Ca^{2+} transients independently from those of ICC-LCs (Fig. 5D and E). It should be noted that the frequencies of USMC Ca^{2+} transients was never lower
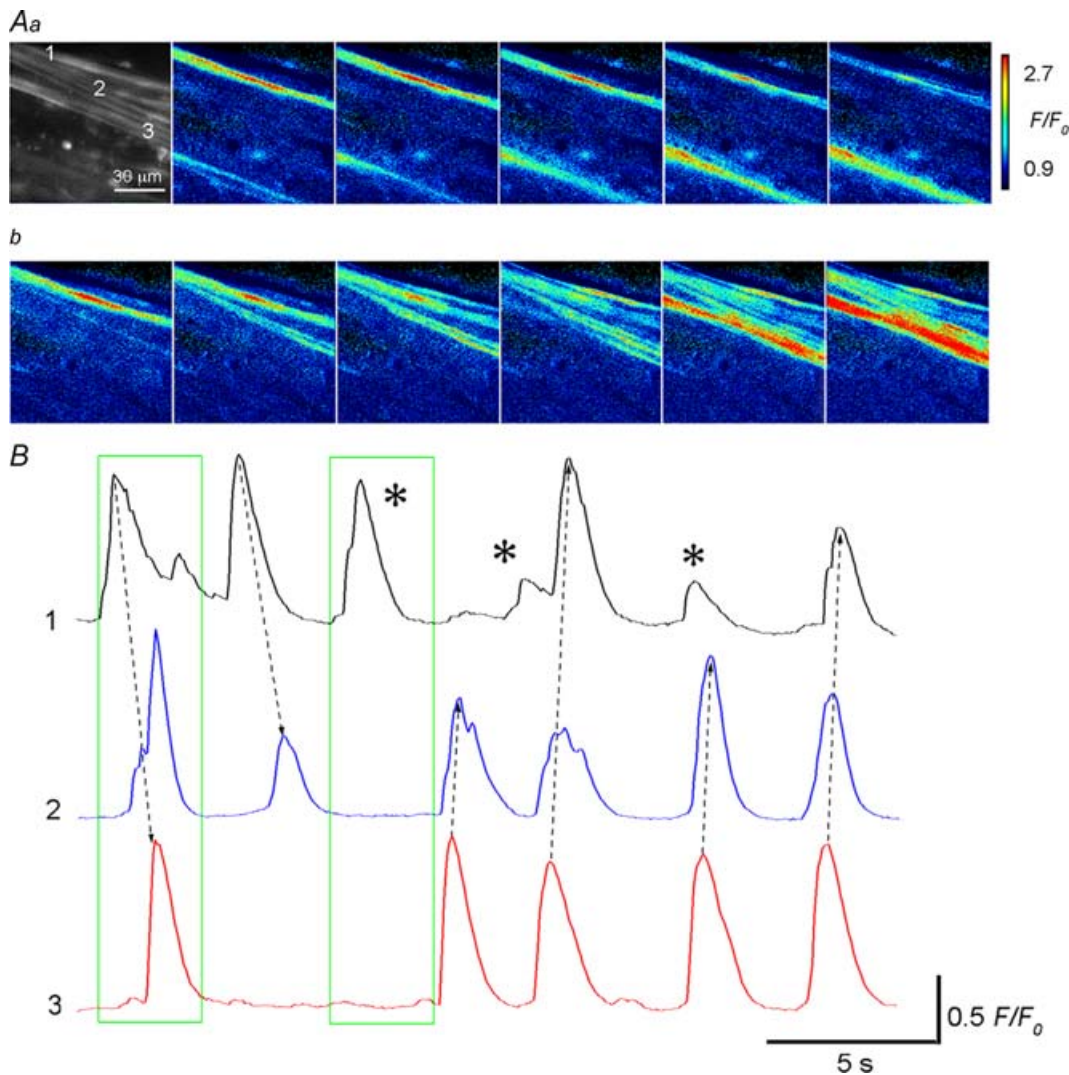
Figure 2. Spontaneous Ca^{2+} transients recorded from USMCs in the rabbit urethra
Aa, a series of frames at intervals of 0.1 s demonstrating two non-propagating Ca^{2+} transients generated by USMCs within a muscle bundle. *b*, another series of frames at intervals of 0.1 s demonstrate an intercellular Ca^{2+} wave within the same smooth muscle bundle. *B*, Ca^{2+} transients initiated in USMC (1) sometimes spread across a muscle bundle to trigger Ca^{2+} transients in USMC (3) and vice versa. On other occasions the Ca^{2+} wave stopped at USMC (2) or did not propagate at all (asterisks). Numbers for traces in *B* correspond to those in *Aa*. The first and second frames correspond to images in *Ab* and *Aa*, respectively. Dotted arrows indicate the direction of Ca^{2+} wave propagation.

than those of ICC-LCs, and that synchronicity between USMCs and ICC-LCs was invariably observed at the lowest frequency of USMC Ca^{2+} transients (Fig. 5*F*).

Role of L-type Ca^{2+} channels in generating Ca^{2+} transients in ICC-LCs and USMCs

Nicardipine (1 μM) abolished ($n = 4$) or greatly reduced the amplitude of Ca^{2+} transients in USMCs (from $0.46 \pm 0.25\ F/F_0$ to $0.066 \pm 0.014\ F/F_0$, $n = 6$, Fig. 6*Aa* and *b*). In preparations which had been treated with nicardipine (1 μM), nicardipine-resistant Ca^{2+} transients occurred at a frequency of $12.3 \pm 3.9\ min^{-1}$ ($10.8 \pm 4.0\ min^{-1}$ in control, $P > 0.05$) and had a half-width 0.51 ± 0.12 s (0.69 ± 0.22 s in control, $P > 0.05$).

As summarized in Fig. 6*C*, nicardipine (1 μM) did not significantly alter the amplitude of Ca^{2+} transients of ICC-LCs ($0.63 \pm 0.18\ F/F_0$ in control,
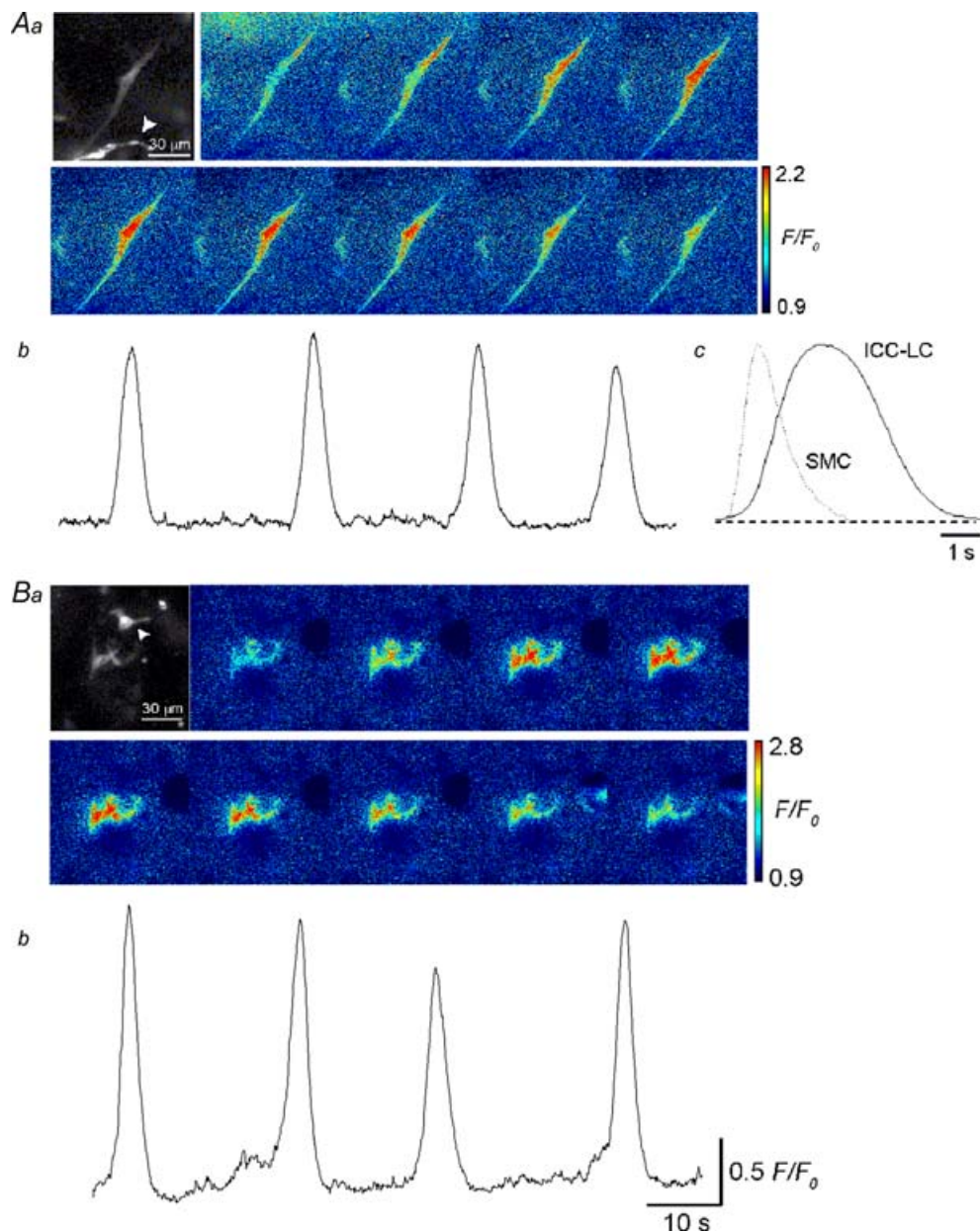
Figure 3. Spontaneous Ca^{2+} transients recorded from ICC-LCs *in situ* in the rabbit urethra
Aa, a series of frames at interval 1 s demonstrating Ca^{2+} transients recorded from a spindle-shaped ICC-LC. *b*, the ICC-LC generated four spontaneous Ca^{2+} transients over 90 s. *c*, averaged Ca^{2+} transients recorded from ICC-LCs had much longer durations than those of the overlaid averaged USMC Ca^{2+} transients. *Ba*, another series of frames at intervals of 1 s demonstrate Ca^{2+} transients recorded from a pair of stellate-shaped ICC-LCs. *b*, in the same preparation, ICC-LCs generated four spontaneous Ca^{2+} transients over 90 s. Note that prominently bright ICC-LCs (arrowheads in *Aa* and *Ba*) did not exhibit any Ca^{2+} signals.

0.61 ± 0.15 F/F_0 in nicardipine, $n = 9$, $P > 0.05$, Fig. 6*Ba* and *b*), nor reduce their frequency (3.7 ± 1.8 min^{-1} in control, 3.2 ± 1.2 min^{-1} in nicardipine, $n = 9$, $P > 0.05$) or half-width (4.1 ± 1.8 s in control, 3.8 ± 0.86 s in nicardipine, $n = 9$, $P > 0.05$).

Since the blockade of L-type Ca^{2+} channels did not suppress Ca^{2+} transients in ICC-LCs, subsequent experiments on ICC-LC Ca^{2+} transients were carried out in the presence of nicardipine ($1\,\mu$M) unless otherwise stated to further diminish muscle contractions.

Role of intracellular Ca^{2+} stores in generating Ca^{2+} transients of ICC-LCs and USMCs

Irrespective of the presence ($n = 6$) or absence ($n = 4$) of nicardipine ($1\,\mu$M), ICC-LC Ca^{2+} transients were abolished by CPA ($10\,\mu$M) within 5 min, indicating that ICC-LC Ca^{2+} transients rely on Ca^{2+} release from intracellular stores (Fig. 7*A*). CPA also increased the basal Ca^{2+} level by 0.28 ± 0.12 F/F_0 ($n = 10$).

CPA ($10\,\mu$M) abolished USMC Ca^{2+} transients within 5 min in seven preparations (Fig. 7*B*). In the remaining five preparations, CPA reduced the frequency of USMC Ca^{2+} transients but did not prevent their generation (Fig. 7*Ca* and *b*). In preparations which had been treated with CPA ($10\,\mu$M) for 45 min, USMC Ca^{2+} transients were generated at a frequency of 2.3 ± 0.46 min^{-1} (9.7 ± 2.6 min^{-1} in control, $P < 0.05$, $n = 5$), and had an amplitude of 0.29 ± 0.089 F/F_0 (0.52 ± 0.11 F/F_0 in control, $P < 0.05$) and a half-width of 1.8 ± 0.52 s (0.63 ± 0.13 s in control, $P < 0.05$). CPA also increased basal Ca^{2+} levels by 0.25 ± 0.11 F/F_0 ($n = 12$).
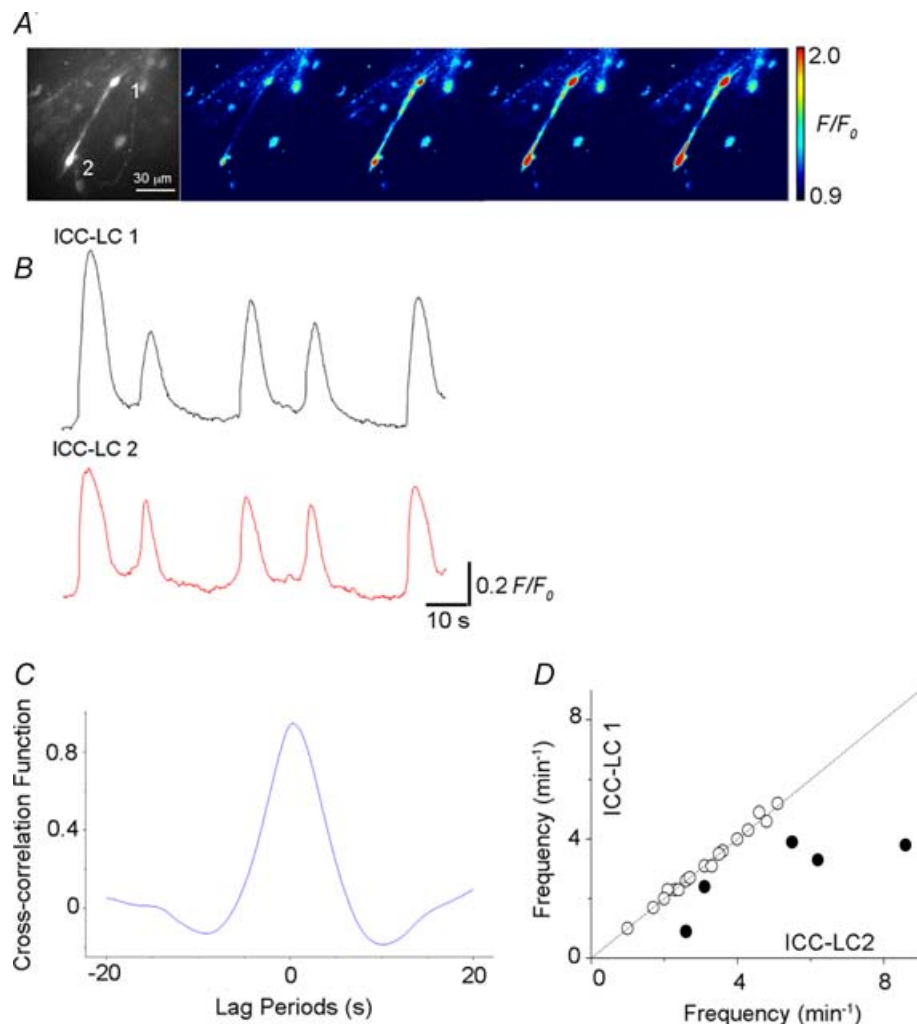
Figure 4. Analysis of the temporal relationship of Ca^{2+} transients between a pair of ICC-LCs
A, a series of frames at intervals of 1 s demonstrating a pair of ICC-LCs (1 and 2) generating spontaneous Ca^{2+} transients. *B*, in the same preparation synchronous Ca^{2+} transients were generated by a pair of ICC-LCs. *C*, a cross-correlogram for this pair of ICC-LCs had a peak near lag period zero. *D*, a comparison of mean frequency between pairs of ICC-LCs showed a close temporal correlation between ICC-LCs for 17 of the 22 pairs of ICC-LCs investigated (○) but not for the remaining five pairs of ICC-LCs (●).
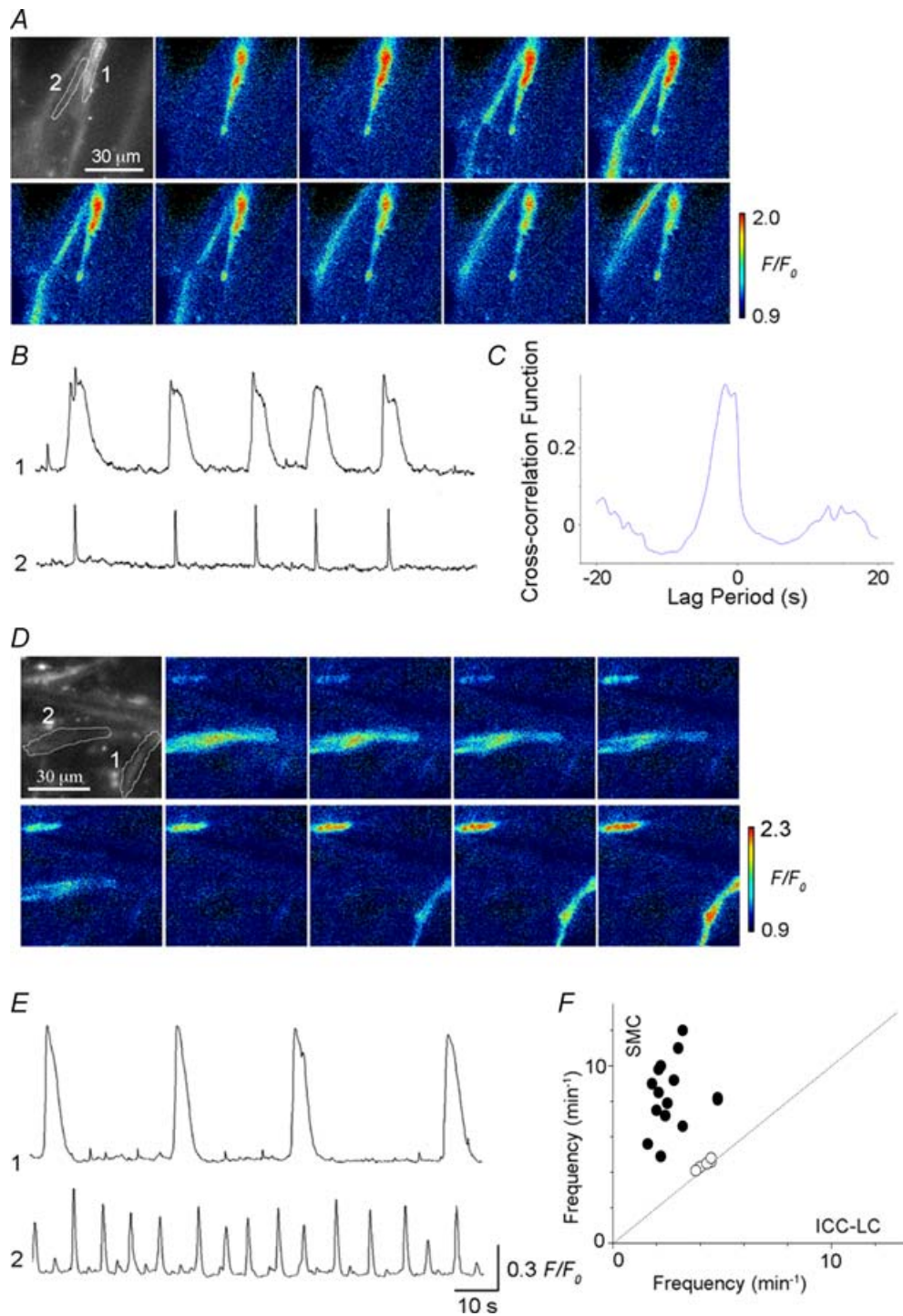
Figure 5. Analysis of the temporal relationship of Ca^{2+} transients between ICC-LCs and USMCs
Aa, a series of frames at intervals of 0.2 s demonstrating USMC Ca^{2+} transients originating from an ICC-LC. *B*, in the same preparation, synchronous Ca^{2+} transients were generated by an ICC-LC (1) and USMC (2). *C*, a cross-correlogram for ICC-LCs and USMCs showed a peak near lag period zero. *D*, in a different preparation, a series of frames at intervals of 0.2 s demonstrating USMC Ca^{2+} transient and subsequent Ca^{2+} transient in a pair of ICC-LCs. *E*, Ca^{2+} transients in ICC-LCs (1) occurred independently from those of USMCs (2). Scale bars also apply to traces in *B*. Numbers for traces in *B* and *E* correspond to those in *A* and *D*. *F*, a comparison of mean frequency between ICC-LCs and USMCs demonstrates a close temporal correlation between the two types of cells in five preparations but not in the remaining 16 preparations.

Role of extracellular Ca^{2+} in generating Ca^{2+} transients of ICC-LCs

Although ICC-LC Ca^{2+} transients were insensitive to nicardipine, increasing $[Ca^{2+}]_o$ from 2.5 mM to 5 mM accelerated their generation (Fig. 8A). In high Ca^{2+} solution, ICC-LC Ca^{2+} transients were generated at a frequency of $9.1 \pm 2.1 \, min^{-1}$ ($3.5 \pm 1.3 \, min^{-1}$ in control, $P < 0.05$, $n = 5$), and had an amplitude of $0.53 \pm 0.1 \, F/F_0$ ($0.76 \pm 0.17 \, F/F_0$ in control, $P < 0.05$) and a half-width of $2.9 \pm 0.35 \, s$ ($3.6 \pm 0.79 \, s$ in control, $P < 0.05$). High Ca^{2+} solution also increased basal Ca^{2+} levels by $0.19 \pm 0.09 \, F/F_0$ ($n = 5$).

In contrast, switching from normal PSS to nominally Ca^{2+} free solution immediately prevented their generation ($n = 4$, Fig. 8B) and also reduced basal Ca^{2+} levels by $0.22 \pm 0.09 \, F/F_0$ ($n = 4$). These results indicated that the generation of ICC-LC Ca^{2+} transients requires a supply of Ca^{2+} from extracellular space through a pathway other than L-type Ca^{2+} channels.

Effects of ryanodine, caffeine and 2-APB in generating Ca^{2+} transients of ICC-LCs

Since Ca^{2+} release from intracellular stores is involved in the generation of ICC-LC Ca^{2+} transients, the contributions due to ryanodine and InsP$_3$ receptors were investigated. Ryanodine (50 μM) first reduced the amplitude of spontaneous Ca^{2+} transients recorded in ICC-LCs, and subsequently prevented their generation within 5 min (Fig. 9A) in association with an increase in basal Ca^{2+} levels by $0.15 \pm 0.07 \, F/F_0$ ($n = 5$). In contrast, caffeine (10 mM) initially increased the frequency of spontaneous Ca^{2+} transients in ICC-LCs and reduced their amplitude. Subsequently it abolished the generation of ICC-LC Ca^{2+} transients within 5 min ($n = 4$, Fig. 9B) and this was accompanied by an increase in basal Ca^{2+} levels by $0.19 \pm 0.08 \, F/F_0$ ($n = 4$).

In 5 of 9 preparations, 2-APB (50 μM) reduced the amplitude of spontaneous Ca^{2+} transients in ICC-LCs, and then almost completely suppressed their
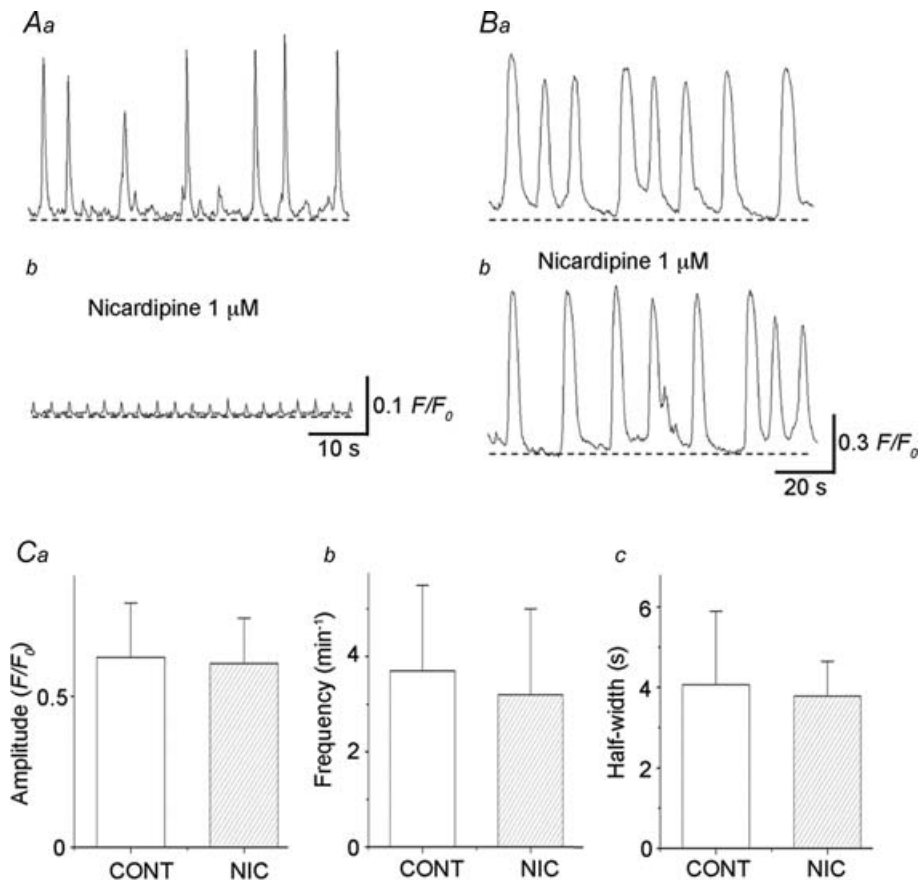
Figure 6. Effects of nicardipine on spontaneous Ca^{2+} transients recorded from USMCs and ICC-LCs in the urethra
Aa, spontaneous Ca^{2+} transients recorded form USMCs of the rabbit urethra were strongly suppressed by nicardipine (1 μM) (*Ab*). *Ba*, in another preparation, ICC-LC Ca^{2+} transients generated spontaneous Ca^{2+} transients which were not inhibited by nicardipine (1 μM) (*Bb*). *C*, summary of the effects of nicardipine on ICC-LC Ca^{2+} transients. Nicardipine (1 μM) did not significantly change amplitude (*a*), frequency (*b*) or half-width (*c*) of ICC-LC Ca^{2+} transients.

generation within 10 min (Fig. 9*C*). In the remaining four preparations, 2-APB reduced the amplitude of ICC-LC Ca^{2+} transients. In four preparations which had been treated with 2-APB (50 μM) for 20 min, ICC-LC Ca^{2+} transients occurred at a frequency of 3.6 ± 2.8 min^{-1} (2.8 ± 2.1 min^{-1} in control, $P > 0.05$, $n = 4$), and had an amplitude of 0.21 ± 0.081 F/F_0 (0.55 ± 0.17 F/F_0 in control, $P < 0.05$) and half-width of 2.4 ± 0.3 s (3.0 ± 0.3 s in control, $P < 0.05$). 2-APB also increased the basal Ca^{2+} level by 0.11 ± 0.05 F/F_0 ($n = 9$).

Role of nitrergic and α-adrenergic simulation in modulating Ca^{2+} transients of ICC-LCs

To investigate whether ICC-LCs *in situ* may be capable of responding to nitrergic and α-adrenergic stimulation during neuromuscular transmission in the urethra, the effects of SIN-1, which decays to release NO (Feelisch *et al.* 1989), and phenylephrine on ICC-LC Ca^{2+} transients were also examined.

SIN-1 (10 μM) reduced the amplitude of ICC-LC Ca^{2+} transients ($n = 6$, Fig. 10*A*) or abolished their generation ($n = 2$). In six preparations which had been treated with SIN-1 for 15 min, ICC-LC Ca^{2+} transients occurred at a frequency of 3.9 ± 1.4 min^{-1}, and had a half-width of 3.4 ± 1.1 s and amplitude of 0.28 ± 0.12 F/F_0. These results were summarized in Fig. 10*B*, and demonstrate that SIN-1 inhibits ICC-LC Ca^{2+} transients by reducing their amplitude.

In contrast, bath applied phenylephrine (1 μM) increased the frequency of ICC-LC Ca^{2+} transients (from 3.5 ± 0.9 min^{-1} to 13.2 ± 3.4 min^{-1}, $P < 0.05$, $n = 4$) and caused a rise in the Ca^{2+} level (0.21 ± 0.08 F/F_0, $n = 4$, Fig. 10*Ca*). Phenylephrine (1 μM) also reduced
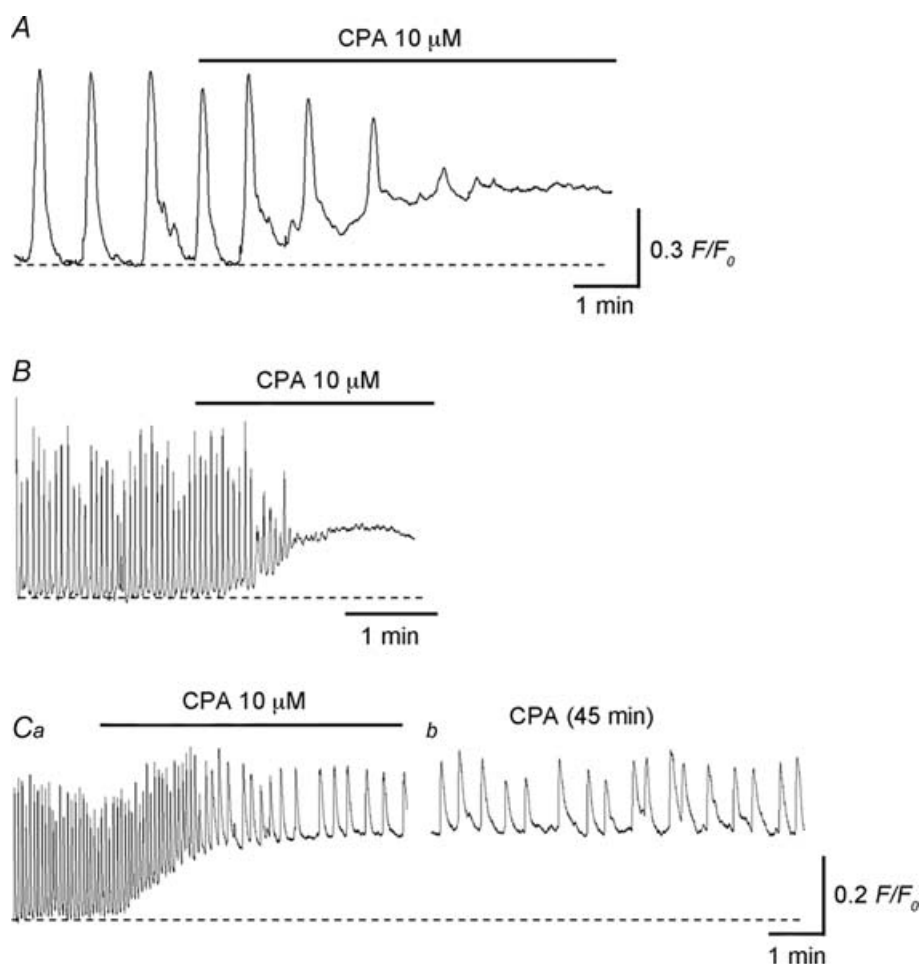
Figure 7. Role of intracellular Ca^{2+} stores in generating spontaneous Ca^{2+} transients in ICC-LCs and USMCs of the urethra
CPA (10 μM) abolished spontaneous Ca^{2+} transients recorded from ICC-LC (*A*) and USMC (*B*). *A* and *B* were recorded from different preparations. *Ca*, in other preparations, CPA reduced the frequency of spontaneous Ca^{2+} transients recorded from USMCs. *b*, in the same preparations which had been treated with CPA for 45 min, spontaneous Ca^{2+} transients occurred but with a markedly reduced frequency and amplitude.

A
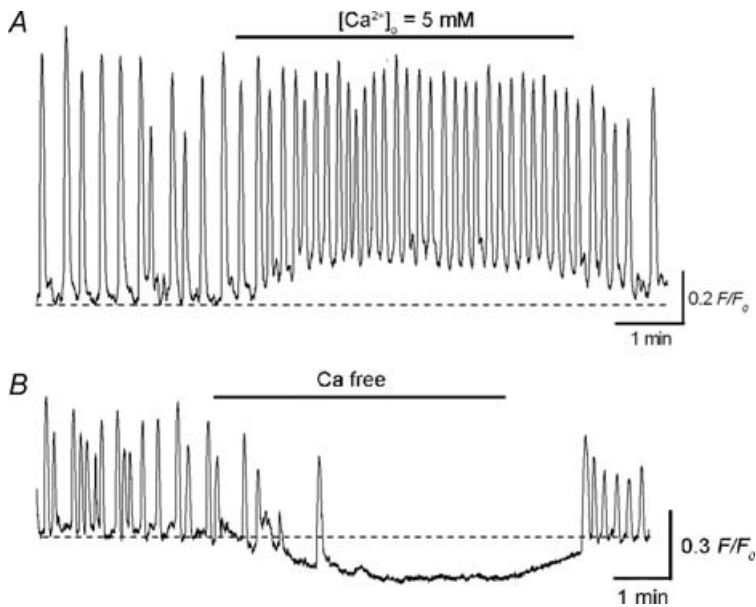
Figure 8. Role of extracellular Ca²⁺ in generating spontaneous Ca²⁺ transients in ICC-LCs of the urethra
A, in a urethral smooth muscle preparation, ICC-LC generated spontaneous Ca²⁺ transients. Increasing $[Ca^{2+}]_o$ from 2.5 mM to 5 mM accelerated ICC-LC Ca²⁺ transients and increased basal Ca²⁺ concentration. *B*, in a different preparation, ICC-LC generated spontaneous Ca²⁺ transients. Switching from normal PSS to nominally Ca²⁺ free solution rapidly abolished ICC-LC Ca²⁺ transients.

the amplitude (from $0.63 \pm 0.12\ F/F_0$ to $0.27 \pm 0.09\ F/F_0$, $P < 0.05$, $n = 4$) and half-width (from 3.4 ± 0.7 s to 1.4 ± 0.3 s, $P < 0.05$, $n = 4$) of ICC-LC Ca²⁺ transients.

A higher concentration of phenylephrine (10 μM) increased the frequency of ICC-LC Ca²⁺ transients, which resulting in a sustained rise in the Ca²⁺ level ($0.31 \pm 0.12\ F/F_0$, $n = 4$, Fig. 10*Cb*), indicating that
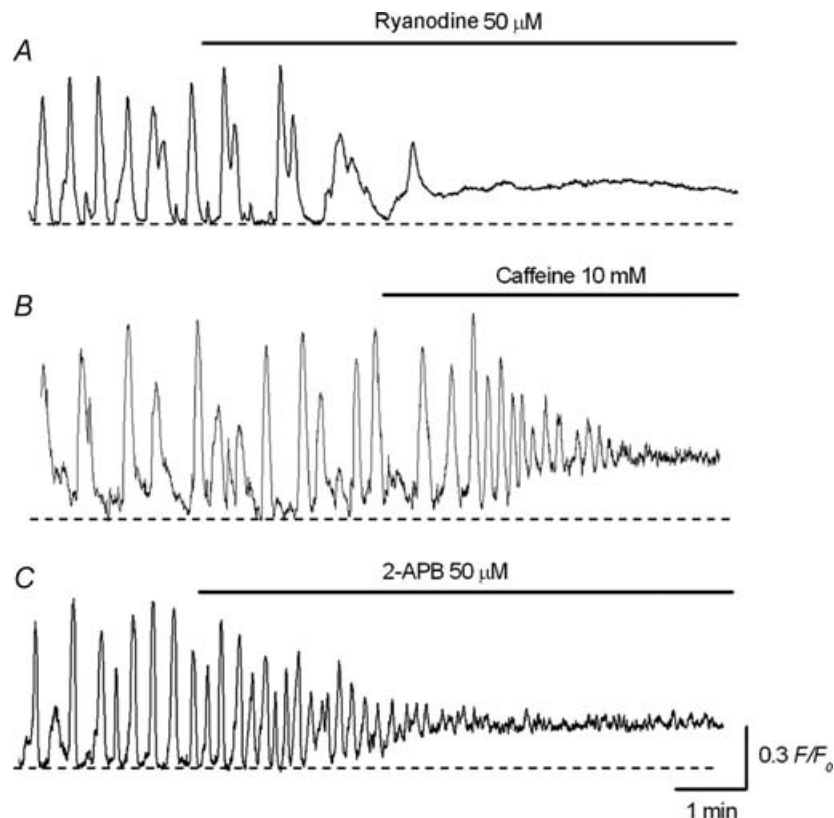

Figure 9. Effects of ryanodine, caffeine and 2-APB on spontaneous Ca²⁺ transients in urethral ICC-LCs
A, ryanodine (50 μM) prevented the generation of spontaneous Ca²⁺ transients recorded in ICC-LCs. *B*, in another preparation, caffeine (10 mM) initially increased the frequency, and then abolished the discharge of spontaneous Ca²⁺ transients recorded in ICC-LC. *C*, in a different preparation, 2-APB (50 μM) greatly suppressed ICC-LC spontaneous Ca²⁺ transients.

ICC-LCs are capable of responding to α-adrenergic stimulation by increasing their frequency of Ca^{2+} transient discharge.

Discussion

Spontaneous Ca^{2+} transients in ICC-LCs recorded in the rabbit urethra *in situ* were insensitive to nicardipine,

an L-type Ca^{2+} channels blocker, which strongly suppressed Ca^{2+} transients in USMCs. Instead these Ca^{2+} transients were dependent on the Ca^{2+} release from intracellular Ca^{2+} stores. At the concentration used in the present study (50 μM), ryanodine could produce a closed state of ryanodine receptor Ca^{2+} channels to inhibit Ca^{2+} release from intracellular stores (Sutko *et al.* 1997).
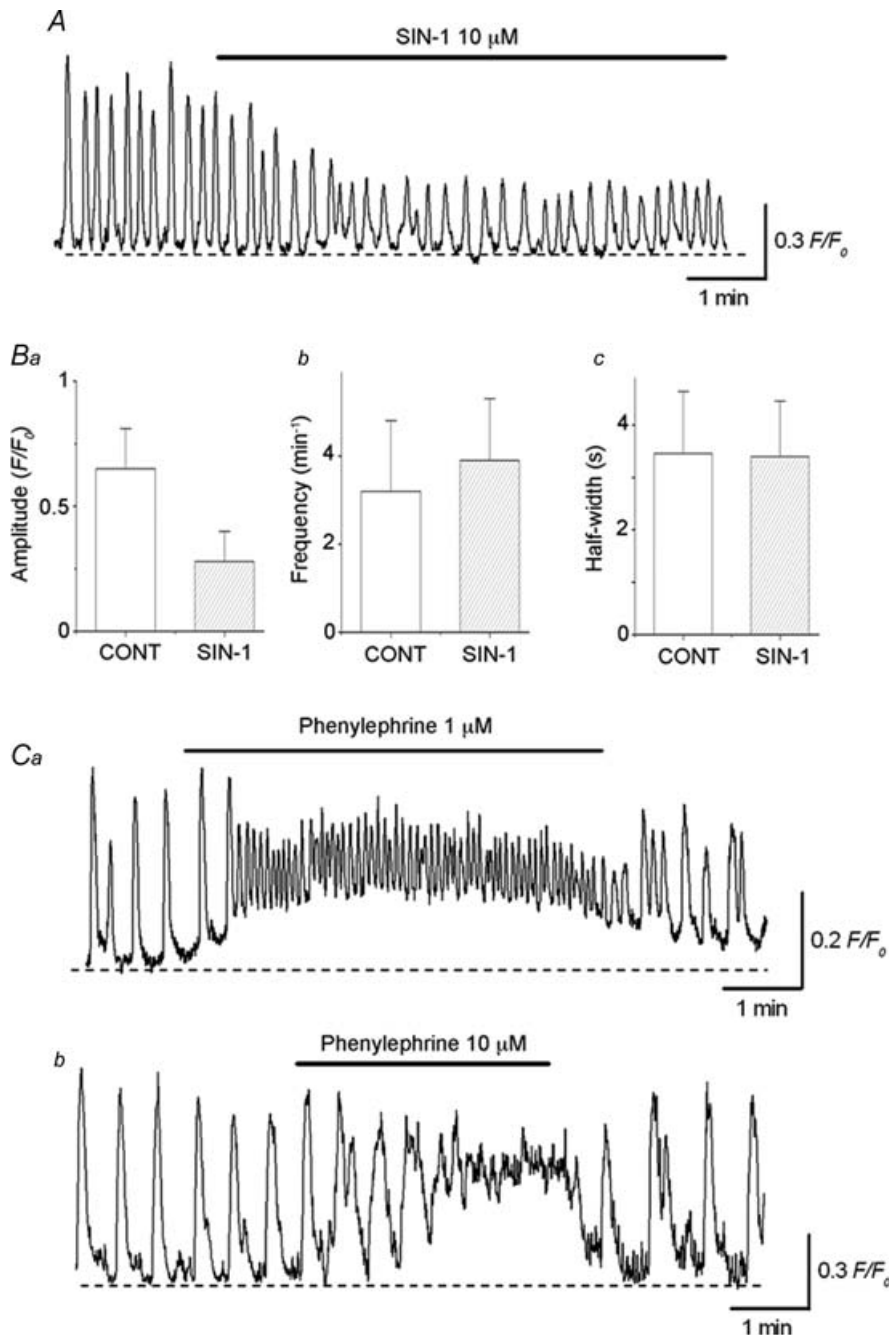
Figure 10. Role of nitrergic and α-adrenergic stimulation in the modulation of spontaneous Ca^{2+} transients recorded from the urethral ICC-LCs
SIN-1 (10 μM; *A*) reduced the amplitude (*Ba*) of spontaneous Ca^{2+} transients recorded from ICC-LC, but did not significantly alter either their frequency (*Bb*) or half-width (*Bc*). *Ca*, in another preparation, bath-applied phenylephrine (1 μM) increased the frequency of spontaneous Ca^{2+} transients recorded from ICC-LC and raised basal Ca^{2+} levels. *b*, a higher concentration of phenylephrine (10 μM) further accelerated ICC-LC Ca^{2+} transients which summed to create a sustained rise in the basal Ca^{2+} concentration.

Indeed, it reduced the amplitude of ICC-LC Ca^{2+} transients before any appreciable rise in basal Ca^{2+} level. In contrast, caffeine increased the frequency of ICC-LC Ca^{2+} transients, suggesting that it may stimulate Ca^{2+} release though the opening of ryanodine receptors. Therefore, ryanodine and caffeine may affect ryanodine receptors in opposite ways, but both eventually prevent the generation of ICC-LCs. However, ryanodine could also increase Ca^{2+} permeability of intracellular stores to decrease the Ca^{2+} store content (Stuko *et al.* 1997). This may account for the continued increase in basal Ca^{2+} levels presumably due to the capacitative Ca^{2+} entry. 2-APB, which has been widely used as a blocker for InsP_3-induced Ca^{2+} release, also suppressed ICC-LC Ca^{2+} transients. These results are in good agreement with studies using isolated ICC-LCs, which revealed that InsP_3 receptors are required to coordinate localized Ca^{2+} transients resulting from ryanodine receptor activation (Sergeant *et al.* 2006*a*). However, 2-APB caused an increase in basal Ca^{2+} which could not be explained by its inhibitory action on InsP_3-induced Ca^{2+} release. Therefore, we cannot exclude the possibility that 2-APB-induced inhibition of ICC-LC Ca^{2+} transients might be attributed to an action on either SERCA (Bilmen *et al.* 2002) or capacitative Ca^{2+} entry (Prakriya & Lewis, 2001).

Although Ca^{2+} transients in ICC-LCs were not diminished by nicardipine, removal of extracellular Ca^{2+} caused an immediate cessation of Ca^{2+} transients, suggesting that Ca^{2+} influx from the extracellular space may be tightly coupled with Ca^{2+}-induced Ca^{2+} release via ryanodine receptors to initiate Ca^{2+} transients in ICC-LCs. This is again consistent with the results obtained from freshly isolated ICC-LCs in the rabbit urethra, in which spontaneous Ca^{2+} oscillations depend on [Ca^{2+}]$_o$ but were not inhibited by nifedipine (Johnson *et al.* 2005). Recently it has been demonstrated that Ca^{2+} entry during the reverse mode activation of the sodium–calcium exchanger (NCX) may be responsible for this Ca^{2+} influx (Bradley *et al.* 2006). One might expect that increased [Ca^{2+}]$_i$ would suppress Ca^{2+} influx through NCX, and thus inhibit ICC-LC Ca^{2+} transients. However, neither a low concentration of phenylephrine nor increasing extracellular Ca^{2+}, which caused substantial increases in [Ca^{2+}]$_i$, prevented the generation of ICC-LC Ca^{2+} transients, suggesting that the inhibition of ICC-LC Ca^{2+} transients by blockers of intracellular Ca^{2+} handling was not due to an increase in [Ca^{2+}]$_i$.

In the present study, the blockade of SERCA with CPA abolished spontaneous Ca^{2+} transients in ICC-LCs, confirming that their generation depends on Ca^{2+} release from intracellular stores. CPA also either abolished USMC Ca^{2+} transients or markedly reduced their frequency, suggesting that ICC-LCs may be responsible for their generation. Since the resting membrane potential of USMCs (between -40 mV and -50 mV)

was close to the threshold of L-type Ca^{2+} channel activation (Hashitani *et al.* 1996), it is likely that the excitability of USMCs in CPA-treated preparations was increased by either membrane depolarizations or raised basal Ca^{2+} level. However, we could not exclude the possibility that a small population of USMCs may be capable of generating spontaneous activity by Ca^{2+} store-independent mechanisms as do detrusor smooth muscle cells (Hashitani *et al.* 2004) after disruption of the 'primary' ICC-LC pacemaker. Alternatively, heterogeneous subpopulations of ICC-LCs with different sensitivities to CPA might exist.

Since ICC-LCs are capable of responding to both nitrergic and α-adrenergic stimulation, ICC-LCs may be targeted by autonomic nerves which play an essential role in generating both contraction and relaxation of the urethral smooth muscle wall (Andersson & Wein, 2004). Indeed spinous-formed cells expressing cGMP immunoreactivity form a network surrounding smooth muscle bundles particularly in the longitudinal smooth muscle layer (Waldeck *et al.* 1998). However, CPA-treated urethral smooth muscles are also able to respond to both nitrergic and α-adrenergic stimulation, suggesting that USMCs may also be directly involved in neuromuscular transmission (Hashitani *et al.* 2006). Unlike bladder in which cyclic GMP (cGMP) was increased in ICC-LCs but not in detrusor smooth muscle cells, addition of a NO donor caused uniform increases in cGMP in USMCs (Smet *et al.* 1996), indicating that they are capable of responding to NO. This paper also demonstrated that nitric oxide synthase-immunoreactive nerve terminals provide a dense innervation to USMCs. This perhaps suggests that neuromuscular transmission in the urethra may not be exclusively targeting ICC-LCs.

One of the major aims of this study was to investigate the temporal correlation between ICC-LCs and USMCs in generating spontaneous activity in the urethra. In the guinea-pig gastric antrum (Hennig *et al.* 2004) and mouse ileum (Park *et al.* 2006), spontaneous Ca^{2+} waves initiated from ICC-MY spread through the ICC-MY network and activated muscle layers. Simultaneous recordings of muscle tension, Ca^{2+} and membrane potential of the gastric antrum demonstrate that all signals occur at the same frequency and duration, indicating that pacemaking electrical activity generated by ICC-MY directly triggers smooth muscle contraction (Dickens *et al.* 2000). ICC-LCs in the urethra often exhibited synchronous Ca^{2+} transients, suggesting that ICC-LCs within a small cluster may be electrically well-coupled. However, ICC-LCs did not form an extensive network (see Lyons *et al.* 2007), nor did their Ca^{2+} transients consistently exhibit a temporal correlation with neighbouring USMCs' Ca^{2+} transients.

The frequency of USMC Ca^{2+} transients was never lower than that of ICC-LCs; synchronicity between USMCs and ICC-LCs also consistently occurred at the lowest frequency

of USMC Ca^{2+} transients. If multiple ICC-LCs including those located out of the field of view or beyond the plane of focus were connected to a smooth muscle bundle within a well coupled electrical syncytium, excitation arising from USMCs or ICC-LCs should be transmitted in both directions equally well so that the frequency of Ca^{2+} transients in ICC-LCs and USMCs should not be very different. However, USMCs often generated non-propagating Ca^{2+} transients, suggesting that cell-to-cell coupling between USMCs may be relatively weak and that USMCs can generate Ca^{2+} transients themselves without input from ICC-LCs. Furthermore, we were not able to demonstrate any correlation between muscle contractions and USMC Ca^{2+} transients, although they occurred at a similar frequency. It seems most likely that individual ICC-LCs are driving USMC bundles independently of other ICC-LCs. In addition, ICC-LCs might have a longer refractory period than USMCs, which may account for their slower time course. We envisage that randomly occurring Ca^{2+} transients in urethral ICC-LCs increase USMC excitability within individual muscle bundles and that the tensions in these bundles sum to produce a sustained contraction of the urethral wall to maintain urinary continence (Bridgewater *et al.* 1993).

ICC-LCs have now been identified throughout the urinary tract, although their physiological functions are still to be elucidated (Hashitani 2006). Interestingly, spontaneous Ca^{2+} transients recorded from ICC-LCs in both suburotherial layer (Wu *et al.* 2004) and detrusor smooth muscle layers (Hashitani *et al.* 2004) of the bladder have low frequencies (about $0.5–2.5\,min^{-1}$) and long durations (some 15 s) as do ICC-LCs in the urethra. However, in the bladder spontaneous Ca^{2+} transients recorded from detrusor ICC-LCs occur independently of those in the smooth muscle cells arising from the spontaneous generation of action potentials (Hashitani *et al.* 2004). Moreover, single ICC-LCs of the mouse renal pelvis, where atypical smooth muscle cells may initiate spontaneous action potential discharge (Lang *et al.* 2006), generate large, long (10 s) inward currents at a low frequency ($1–3\,min^{-1}$). ICC-LCs in the urethra may consist of distinct subpopulations, where some ICC-LCs with a relatively fast time course may act as electrical pacemakers, whilst others with a slower time course may play another supportive role. In mouse ileum, a sub-population of ICC-MY display spontaneous Ca^{2+} transients which fire at a low frequency and do not appear to drive smooth muscle Ca^{2+} transients (Yamazawa & Iino, 2002).

In conclusion, properties of ICC-LCs *in situ* in the rabbit urethra are very similar to those of isolated ICC-LCs, suggesting that they may act as a primary pacemaker in generating spontaneous contractions. However, signal transmission from ICC-LCs to USMCs may be much less extensive than that between ICC and smooth muscle cells in the GI tract, and thus electrical pacemaking signals generated by ICC-LCs may be 'less securely' transmitted to smooth muscles.

References

Andersson K-E & Wein AJ (2004). Pharmacology of the lower urinary tract: basis for current and future treatments of urinary incontinence. *Pharmacol Rev* **56**, 581–631.

Bilmen JG, Wootton LL, Godfrey RE, Smart OS & Michelangeli F (2002). Inhibition of SERCA Ca^{2+} pumps by 2-aminoethoxydiphenyl borate (2-APB). 2-APB reduces both Ca^{2+} binding and phosphoryl transfer from ATP, by interfering with the pathway leading to the Ca^{2+}-binding sites. *Eur J Biochem* **269**, 3678–3687.

Bradley E, Hollywood MA, Johnston L, Large RJ, Matsuda T, Baba A, McHale NG, Thornbury KD & Sergeant GP (2006). Contribution of reverse Na^+–Ca^{2+} exchange to spontaneous activity in interstitial cells of Cajal in the rabbit urethra. *J Physiol* **574**, 651–661.

Bridgewater M, Macneill HF & Brading AF (1993). Regulation of urethral tone in pig urethral smooth muscle. *J Urol* **150**, 223–228.

Dickens EJ, Hirst GDS & Tomica T (1999). Identification of rhythmically active cells in guineapig stomach. *J Physiol* **514**, 513–531.

Dickens EJ, Edwards FR & Hirst GDS (2000). Vagal inhibition in the antral region of guinae pig stomach. *Am J Physiol Gastrointest Liver Physiol* **279**, G388–G399.

Feelisch M, Ostrowski J & Noack E (1989). On the mechanism of NO release from sydnonimines. *J Cardiovasc Pharmacol* **14** (Suppl. 11), S13–S22.

Hashitani H (2006). Interaction between interstitial cells and smooth muscles in the lower urinary tract and penis. *J Physiol* **576**, 707–714.

Hashitani H & Edwards FR (1999). Spontaneous and neurally activated depolarizations in smooth muscle cells of the guinea-pig urethra. *J Physiol* **514**, 459–470.

Hashitani H, Fukuta H, Takano H, Klemm MF & Suzuki H (2001). Origin and propagation of spontaneous excitation in smooth muscle of the guinea-pig urinary bladder. *J Physiol* **530**, 273–286.

Hashitani H, Van Helden DF & Suzuki H (1996). Properties of spontaneous depolarizations in circular smooth muscle cells of rabbit urethra. *Br J Pharmacol* **118**, 1627–1632.

Hashitani H, Yanai Y, Kohri K & Suzuki H (2006). Heterogeneous CPA sensitivity of spontaneous excitation in smooth muscle of the rabbit urethra. *Br J Pharmacol* **148**, 340–349.

Hashitani H, Yanai Y & Suzuki H (2004). Role of interstitial cells and gap junctions in the transmission of spontaneous Ca^{2+} signals in detrusor smooth muscles of the guinea-pig urinary bladder. *J Physiol* **559**, 567–581.

Hennig GW, Hirst GD, Park KJ, Smith CB, Sanders KM, Ward SM & Smith TK (2004). Propagation of pacemaker activity in the guinea-pig antrum. *J Physiol* **556**, 585–599.

Johnston L, Sergeant GP, Hollywood MA, Thornbury KD & McHale NG (2005). Calcium oscillations in interstitial cells of the rabbit urethra. *J Physiol* **565**, 449–461.

Lang RJ, Tonta MA, Zoltkowski BZ, Meeker WF, Wendt I & Parkington HC (2006). Pyeloureteric peristalsis: role of atypical smooth muscle cells and interstitial cells of Cajal-like cells as pacemakers. *J Physiol* **576**, 695–705.

Lyons AD, Gardiner TA & McCloskey KD (2007). Kit-positive interstitial cells in the rabbit urethra: structural relationships with nerves and smooth muscle. *BJU Int* **99**, 687–694.

McHale NG, Hollywood MA, Sergeant GP, Shafei M, Thornbury KT & Ward SM (2006). Organization and function of ICC in the urinary tract. *J Physiol* **576**, 689–694.

Park KJ, Hennig GW, Lee HT, Spencer NJ, Ward SM, Smith TK & Sanders KM (2006). Spatial and temporal mapping of pacemaker activity in interstitial cells of Cajal in mouse ileum in situ. *Am J Physiol Cell Physiol* **290**, C1411–C1427.

Prakriya M & Lewis RS (2001). Potentiation and inhibition of Ca²⁺ release-activated Ca²⁺ channels by 2-aminoethyldiphenyl borate (2-APB) occurs independently of IP₃ receptors. *J Physiol* **536**, 3–19.

Sanders KM, Koh SD & Ward SM (2006*a*). Interstitial cells of Cajal as pacemakers in the gastrointestinal tract. *Annu Rev Physiol* **68**, 307–343.

Sergeant GP, Hollywood MA, McCloskey KD, McHale NG & Thornbury KD (2001). Role of IP₃ in modulation of spontaneous activity in pacemaker cells of rabbit urethra. *Am J Physiol Cell Physiol* **280**, C1349–C1356.

Sergeant GP, Hollywood MA, McCloskey KD, Thornbury KD & McHale NG (2000). Specialised pacemaking cells in the rabbit urethra. *J Physiol* **526**, 359–366.

Sergeant GP, Hollywood MA, McHale NG & Thornbury KD (2006*a*). Ca²⁺ signalling in urethral interstitial cells of Cajal. *J Physiol* **576**, 715–720.

Sergeant GP, Johnston L, McHale NG, Thornbury KD & Hollywood MA (2006*b*). Activation of the cGMP/PKG pathway inhibits electrical activity in rabbit urethral interstitial cells of Cajal by reducing the spatial spread of Ca²⁺ waves. *J Physiol* **574**, 167–181.

Sergeant GP, Thornbury KD, McHale NG & Hollywood MA (2002). Characterization of norepinephrine-evoked inward currents in interstitial cells isolated from the rabbit urethra. *Am J Physiol Cell Physiol* **283**, C885–C894.

Smet PJ, Jonavicius J, Marshall VR & de Vente J (1996). Distribution of nitric oxide synthase-immunoreactive nerves and identification of the cellular targets of nitric oxide in guinea-pig and human urinary bladder by cGMP immunohistochemistry. *Neuroscience* **71**, 337–348.

Sutko JL, Airey JA, Welch W & Ruest L (1997). The pharmacology of ryanodine and related compounds. *Pharmacol Rev* **49**, 53–98.

Suzuki H, Ward SM, Bayguinov YR, Edwards FR & Hirst GDS (2003). Involvement of intramuscular interstitial cells in nitrergic inhibition in the mouse gastric antrum. *J Physiol* **546**, 751–763.

Waldeck K, Ny L, Persson K & Andersson K-E (1998). Mediators and mechanisms of relaxation in rabbit urethral smooth muscle. *Br J Pharmacol* **123**, 617–624.

Ward SM, Beckett EA, Wang X, Baker F, Khoyi M & Sanders KM (2000). Interstitial cells of Cajal mediate cholinergic neurotransmission from enteric motor neurons. *J Neurosci* **20**, 1393–1403.

Wu C, Sui GP & Fry CH (2004). Purinergic regulation of guinea pig suburothelial myofibroblasts. *J Physiol* **559**, 231–243.

Yamazawa T & Iino M (2002). Simultaneous imaging of Ca²⁺ signals in interstitial cells of Cajal and longitudinal smooth muscle cells during rhythmic activity in mouse ileum. *J Physiol* **538**, 823–835.

Acknowledgements